The Korean Journal of Ceramics, **1** [1] 7-12 (1995)

Quantitative Analysis of Ultrathin SiO_2 Interfacial Layer by AES Depth Profiling

Ju Won Soh, Jong Seok Kim and Won Jong Lee

Dept. of Mater. Sci. and Eng., Korea Advanced Institute of Science and Technology, Taejon 305-701, Korea

(Received January 12, 1995)

When a Ta_2O_5 dielectric film is deposited on a bare silicon, the growth of SiO_2 at the Ta_2O_5/Si interface cannot be avoided. Even though the SiO_2 layer is ultrathin (a few nm), it has great effects on the electrical properties of the capacitor. The concentration depth profiles of the ultrathin interfacial SiO_2 and SiO_2/Si_3N_4 layers were obtained using an Auger electron spectroscopy (AES) equipped with a cylindrical mirror analyzer (CMA). These AES depth profiles were quantitatively analyzed by comparing with the theoretical depth profiles which were obtained by considering the inelastic mean free path of Auger electrons and the angular acceptance function of CMA. The direct measurement of the interfacial layer thicknesses by using a high resolution cross-sectional TEM confirmed the accuracy of the AES depth analysis. The SiO_2/Si_3N_4 double layers, which were not distinguishable from each other under the TEM observation, could be effectively analyzed by the AES depth profiling technique.

Key words : AES, Depth profiling, Silicon oxide, Thickness measurement

I. Introduction

The demands for the higher integrity in devices and the lower operating voltage than ever spur the research for developing high dielectric materials to replace Si_3N_4/SiO_2 currently used in DRAM capacitors. Ta_2O_5 film is an attractive candidate for its high dielectric constant (ε_r=25~28) and relatively good leakage current characteristics.[1] In a conventional silicon fabrication process, the charge storage dielectric film is usually deposited on the surface of silicon. When the Ta_2O_5 film is deposited on the bare silicon surface, the simultaneous growth of SiO_2 layer at the Ta_2O_5/Si interface cannot be avoided. Even though the SiO_2 interfacial layer is ultrathin (a few nm), it has great effects on the electrical properties such as leakage current characteristics and dielectric constant of the capacitor. The important influence of the interfacial SiO_2 layer on the dielectric characteristics of the Ta_2O_5/SiO_2 double layer has been pointed out by some other researchers.[2,3] Therefore the exact analysis of the interfacial layer, especially the determination of its thickness, is essential to understand the characteristics of the capacitor.

High resolution cross-sectional transmission electron microscopy (TEM) is mostly used to measure the thickness of the interfacial SiO_2 layer. The cross-sectional TEM work, however, demands time-consuming efforts in preparation of thin foils. It is also difficult to analyze the large area of the specimen and to distinguish the SiO_2 layer from the other amorphous layers. Auger electron spectroscopy (AES) is very suitable for getting a compositional depth profile of a thin film within a reasonable timespan because it has an excellent surface sensitivity and short data acquisition time. Furthermore, no special process in preparing the sample is necessary. However, the depth resolution of the AES depth profiling is limited by the inelastic mean free path of the Auger electron and by the sputtering induced effects, which cause the difficulty in the quantitative analysis of the AES depth profiles.

In this study, the concentration depth profile of the ultrathin SiO_2 layer formed at the Ta_2O_5/Si interface was experimentally obtained using an AES. Its quantitative analysis was accomplished by comparing with the theoretical depth profiles which were obtained by taking into account the inelastic mean free path of Auger electrons and the angular acceptance function of the electron energy analyzer. The thicknesses of the ultrathin SiO_2 layers determined by the AES analysis were compared with those measured directly from the high-resolution cross-sectional TEM micrographs.

II. Experimental

1. Theoretical AES depth profiling

When Auger electrons are generated from element A by an incident high energy electron beam, the Auger peak intensity I can be expressed as eq. (1) under the assumptions that the surface is flat and the material is step-like uniform[4] :

$$I = I_p \sigma P_A T \int C(x) \rho (1+r) \exp\{-x/\lambda \cos\theta\} dx \qquad (1)$$

where C (x) is the local atomic concentration of an element A at depth x, I_p is the primary electron beam current, σ is the ionization cross-section, P_A is the probability that an excited atom will decay through an Auger transition, T is the fraction of Auger electrons detected by the analyzer, ρ is the local atomic density, r is the back scattering factor, λ is the inelastic mean free path (IMFP) of the Auger electron in a given matrix and θ is the emission angle of the detected Auger electron with respect to the normal to the specimen surface. If there is no matrix effect so that ρ and r are constants, eq. (1) is reduced to :

$$I = K\int C(x)\exp\{-x/\lambda\cos\theta\}dx \quad (2)$$

where K is a spectroscopy constant for a fixed beam current and Auger peak. In order to minimize the effects of instrumental and experimental factors, the absolute Auger intensity (I) was normalized with the Auger peak intensity of the pure elemental bulk standard (I°). The normalized intensity R is :

$$R = I/I^\circ = \int C(x)\exp\{-x/\lambda\cos\theta\}dx/\int \exp\{-x/\lambda\cos\theta\}dx \quad (3)$$

The effective escape depth (λcosθ) of the Auger electrons is the most important factor for the calculation of the Auger signal. The IMFP of the Auger electron of element A (in an A_XB_Y molecule) is expressed as $\lambda_{A(A_XB_Y)/C}$ when the electron travels in the matrix C. We calculated the IMFP from the empirical relations suggested by Seah and Dench.[5] The empirical relations are expressed as eq. (4-1) and eq. (4-2) for elements and for inorganic compounds, respectively.

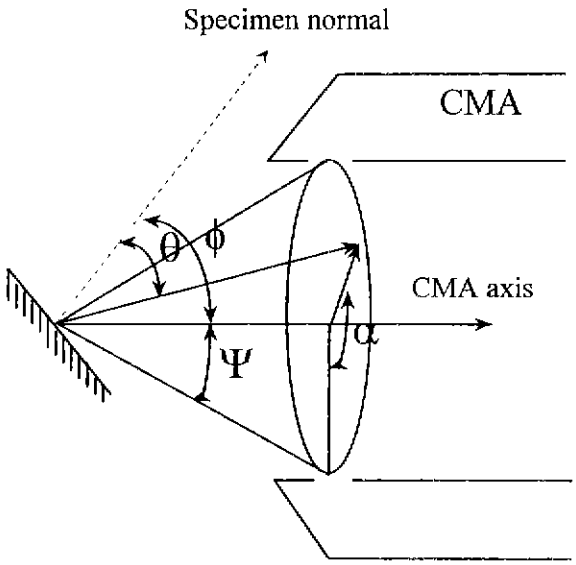

Fig. 1. Geometry of the AES analysis configuration with CMA: ψ, aperture angle of CMA (42.3°) ; ϕ, angle between the surface mormal and the CMA axis (i.e. specimen tilting angle) ; α, azimuth of CMA axis (0° α < 180°) ; θ, emission angle of Auger electrons.

$$\lambda_{A(A_XB_Y)/C} = 538\,A_C\,E_{A(A_XB_Y)}^{-2} + 0.41\,(A_C^{3/2}E_{A(A_XB_Y)})^{1/2} \quad (4\text{-}1)$$

$$\lambda_{A(A_XB_Y)/C} = 2170\,A_C\,E_{A(A_XB_Y)}^{-2} + 0.72\,(A_C^{3/2}E_{A(A_XB_Y)})^{1/2} \quad (4\text{-}2)$$

where $E_{A(A_XB_Y)}$ is the kinetic energy of the Auger electron of element A in an A_XB_Y molecule and A_C is the monolayer thickness of the matrix C.

Cylindrical mirror analyzer (CMA) which consists of two concentric cylinders of different radii was used to analyze the Auger electron energy. CMA has a ring-type acceptance slit to have a large solid acceptance angle. Fig. 1 shows the geometry of CMA with respect to the specimen. The angular acceptance function (cosθ) of CMA is expressed as[6] :

$$\cos\theta = \cos\Psi\cos\phi - \sin\Psi\sin\phi\cos\alpha \quad (5)$$

where θ is the emission angle of Auger electrons, Ψ is the aperture angle (42.3°) of CMA, ϕ is the specimen tilting angle (30° in the present experiment) and α is the azimuth of CMA axis (0° < α < 180°). The azimuth α was divided by 1° and the values of cosθ were calculated according to eq. (5) with those different α values. The normalized Auger intensity R was obtained by averaging all of the relative intensities which were computed from eq. (3) with every cosθ value. The normalized intensity of the Auger electron of element A (in an A_XB_Y molecule) is expressed as $R_{A(A_XB_Y)}$.

2. Experimental Auger depth profiling

Three specimens with the structure of $Ta_2O_5/SiO_2/(Si_3N_4)/Si$ were prepared at the different conditions which are given in Table 1. Ta_2O_5 thin films were deposited on Si or Si_3N_4/Si substrates by the electron cyclotron resonance plasma enhanced chemical vapor deposition (ECR PECVD) method using $Ta(OC_2H_5)_5$ and oxygen as reactant gases. Specimen 1 was prepared by depositing Ta_2O_5 thin film on a bare silicon wafer at 205°C and annealing for 30 minutes at 850°C in an oxygen ambient. The SiO_2 interfacial layer was formed during the deposition of Ta_2O_5 film by the oxygen ECR plasma and grew further during the post-annealing process. Specimen 2 was prepared by depositing Ta_2O_5 thin film on a bare silicon wafer at a low

Table 1. Specimen Preparation Conditions.

	Specimen 1	Specimen 2	Specimen 3
Substrate	Si	Si	Si_3N_4/Si[a]
Ta_2O_5 deposition temperature[b]	205°C	95°C	205°C
Post-annealing	YES[c]	NO	NO

a : Si_3N_4 layer was prepared on Si substrate by ECR plasma nitridation under the following conditions : microwave power 300 W, substrate temperature 205°C and pressure 0.2 mtorr.
b : Ta_2O_5 films were deposited by ECR PECVD method using Ta $(C_2H_5O)_5$ and O_2 at 300 W and 0.5 mtorr.
c : Post-annealed at 850°C for 30 minutes in an O_2 environment of 1 atm.

deposition temperature of 95°C to form a very thin SiO_2 interfacial layer. In case of specimen 3, Ta_2O_5 thin film was deposited on a Si_3N_4/Si substrate at 205°C to form a SiO_2/Si_3N_4 double amorphous interfacial layer. The Si_3N_4/Si substrate was prepared by nitriding a silicon wafer surface in an nitrogen ECR plasma to form an amorphous Si_3N_4 layer about 4 nm thick. Si_3N_4 layer has been used as a buffer layer to suppress the formation of interfacial SiO_2 layer.

The thicknesses of the interfacial SiO_2 or SiO_2/Si_3N_4 layers were precisely measured by using a high-resolution cross-sectional TEM (JEOL, JEM 2000EX) with a point resolution of 0.21 nm. The cross-sectional TEM specimens were prepared by the face-to-face method. The specimens were mechanically polished to a thickness of about 30 μm and then bonded to a copper grid before they were thinned with an ion beam milling machine. Figs. 2(a)-(c) are the cross-sectional TEM micrographs obtained from specimens 1, 2 and 3, respectively. The SiO_2 layer is clearly distinguishable from Ta_2O_5 and Si in the TEM micrographs. The regularly-spaced white points appeared in the lower part of the photograph represent the lattice points of the Si single crystal. The vertical distance from point to point is 0.54 nm which corresponds to the Si (100) interplanar spacing and the horizontal distance is 0.38 nm which corresponds to the Si (110) interplanar spacing. These values enable us to measure the thickness of the interfacial SiO_2 layers very accurately. The measured thicknesses of the interfacial SiO_2 layers of specimen 1 and 2 are 10.9 nm and 3.1 nm respectively. The thickness of the SiO_2/Si_3N_4 double layer of specimen 3 is 4.2 nm. It should be noted that the two amorphous layers are not distinguishable each other under the TEM observation as shown in Fig. 2(c).

The sputtered depth profiles of the interfacial SiO_2 or SiO_2/Si_3N_4 layers were obtained by using a scanning Auger microscopy (Perkin Elmer, PHI 610) equipped with a CMA and a sputtering ion gun. The sputtering and analysis conditions are as follows : specimen tilting angle (ϕ) 30° with respect to the CMA axis, incident electron energy 5 keV, modulation voltage 4 V, Auger analysis area 10×15 μm^2, sputter ion beam energy 3 keV and ion beam current 58.2 μA/cm^2.

For the quantitative analysis of the sputtered depth profiles, the sputter depth scale should be calibrated. The most convenient way to calibrate the sputter depth scale is to measure the time spent for sputtering through a layer of known thickness. Specimen 1 which has the thickest SiO_2 interfacial layer among three specimens was selected as the reference sample to determine the sputtering rate of the SiO_2 layer during AES depth profiling. The thicknesses of the interfacial SiO_2(or Si_3N_4) layers of specimens 2 and 3 measured from the AES sputtered depth profiles were compared with those directly measured from the high-resolution cross-sectional TEM.

III. Results and Discussion

1. Theoretical depth profiles

Theoretical depth profiles of the specimens with the structure of $Ta_2O_5/SiO_2/Si$ were calculated under the assumption of step-like uniform layers. Fig. 3 shows the specimen structure in which the thickness of SiO_2 in-

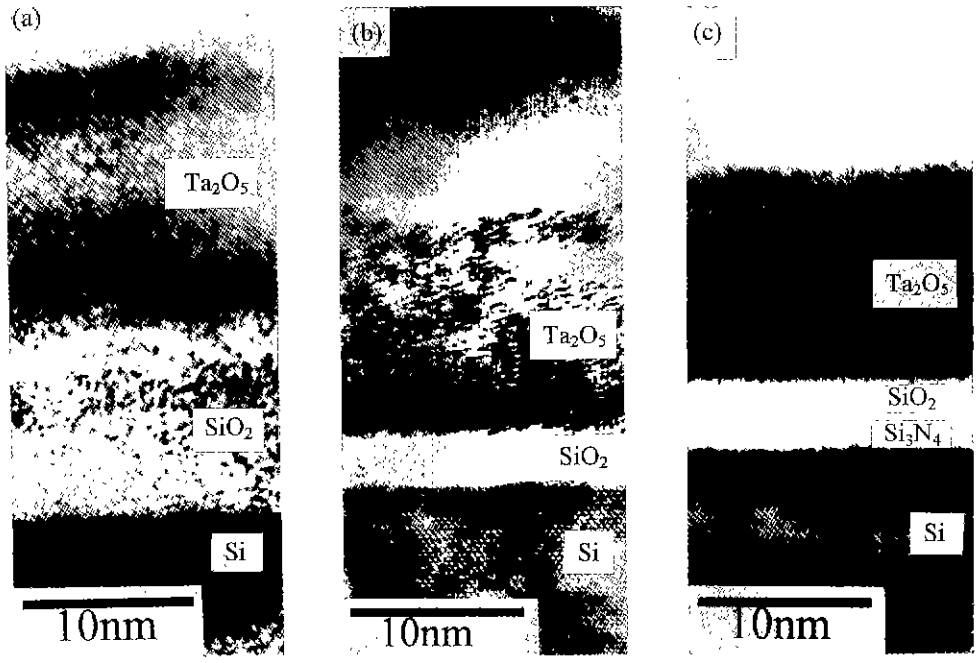

Fig. 2. Cross-sectional TEM micrographs of (a) specimen 1, (b) specimen 2 and (c) specimen 3. Preparation conditions of the specimens are listed in Table 1.

terfacial layer is t. The position X represents the surface of the specimen which is being eroded by ion sputtering. The upper surface of the SiO_2 interfacial layer is set as X =0. The oxygen atoms in Ta_2O_5 were preferentially sputtered and the degree of oxygen deficiency varied with the sputtered depth. Thus, the tantalum oxide film being sputtered is expressed as TaO_X (where $x < 2.5$) instead of Ta_2O_5.

When the tantalum oxide is being eroded (i.e. $X < 0$), $R_{Ta(TaO_X)}$, $R_{Si(SiO_2)}$ and $R_{Si(Si)}$ are expressed as eqs. (6)-(8), respectively.

$$R_{Ta(TaO_X)} = 1 - \exp\{X/\lambda_{Ta(TaO_X)/TaO_X}\cos\theta\} \quad (6)$$

$$R_{Si(SiO_2)} = [1 - \exp\{t/\lambda_{Si(SiO_2)/SiO_2}\cos\theta\}] \exp\{X/\lambda_{Si(SiO_2)/TaO_X}\cos\theta\} \quad (7)$$

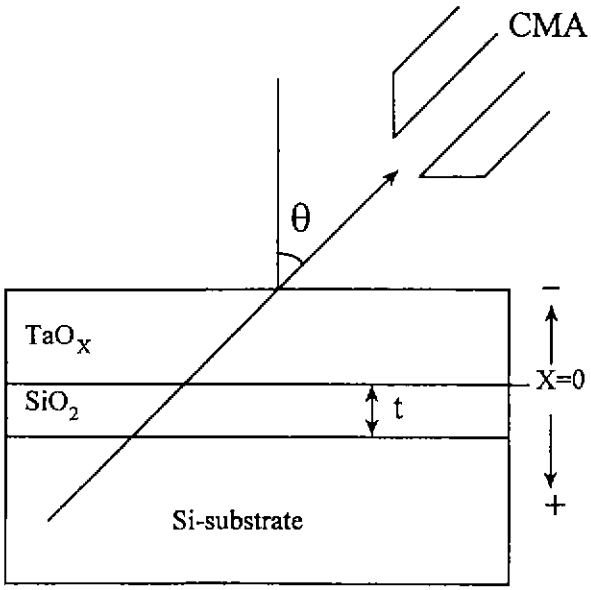

Fig. 3. Schematic diagram for quantitative analysis of AES depth profile.

$$R_{Si(Si)} = \exp\{-t/\lambda_{Si(Si)/SiO_2}\cos\theta\} \exp\{X/\lambda_{Si(Si)/TaO_X}\cos\theta\} \quad (8)$$

where $\lambda_{Ta(TaO_X)}$ is IMFP of Ta MNN Auger electron with 1677 eV, $\lambda_{Si(SiO_2)}$ is IMFP of Si LMM Auger electron with 76 eV and $\lambda_{Si(Si)}$ is IMFP of Si LMM Auger electron with 92 eV. When the interfacial SiO_2 layer is being eroded (i. e. $0 \leq X \leq t$), $R_{Ta(TaO_X)}$ is zero because TaO_X layer is completely eroded. $R_{Si(SiO_2)}$ and $R_{Si(Si)}$ are expressed as eqs. (9) and (10), respectively.

$$R_{Si(SiO_2)} = 1 - \exp\{(t-X)/\lambda_{Si(SiO_2)/SiO_2}\cos\theta\} \quad (9)$$

$$R_{Si(Si)} = \exp\{-(t-X)/\lambda_{Si(Si)/SiO_2}\cos\theta\} \quad (10)$$

When the Si substrate is being eroded (i.e. $X > t$), $R_{Ta(TaO_X)}$ and $R_{Si(SiO_2)}$ are zero and $R_{Si(Si)}$ is one. IMFP values of various Auger electrons were calculated according to the Seah and Dench's method of eq. (4) and tabulated in Table 2. There were two points to be considered in calculating $\lambda_{Ta(TaO_X)/TaO_X}$. The kinetic energy ($E_{Ta(TaO_X)}$) of MNN

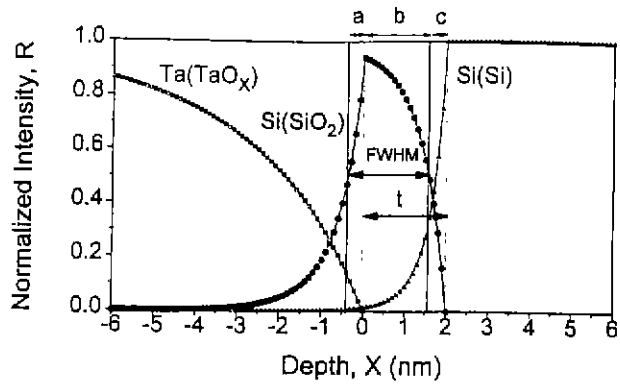

Fig. 4. Theoretical depth profiles of $R_{Ta(TaO_X)}$, $R_{Si(SiO_2)}$ and $R_{Si(Si)}$ calculated assuming ideal microsectioning when the thickness (t) of the interfacial SiO_2 layer is 2.0 nm.
□ : $R_{Ta(TaO_X)}$, ● : $R_{Si(SiO_X)}$, △ : $R_{Si(Si)}$

Table 2. Inelastic Mean Free Paths of the Auger Electrons.

$\lambda_{A(A_XB_Y)/C}$ [a]	Auger electron	$E_{A(A_XB_Y)}$ [b]	Matrix	Monolayer thickness	Calculated value of λ
$\lambda_{Ta(TaO_X)/TaO_X}$	MNN Auger electron of Ta atom in TaO_X	1677 eV	TaO_X	0.246 nm	3.567 nm
$\lambda_{Si(SiO_2)/TaO_X}$	LMM Auger electron of Si atom in SiO_2	76 eV	TaO_X	0.246 nm	0.853 nm
$\lambda_{Si(SiO_2)/SiO_2}$	LMM Auger electron of Si atom in SiO_2	76 eV	SiO_2	0.248 nm	0.868 nm
$\lambda_{Si(Si)/TaO_X}$	LMM Auger electron of Si atom in Si	92 eV	TaO_X	0.246 nm	0.900 nm
$\lambda_{Si(Si)/SiO_2}$	LMM Auger electron of Si atom in Si	92 eV	SiO_2	0.248 nm	0.916 nm
$\lambda_{Si(Si)/Si}$	LMM Auger electorn of Si atom in Si	92 eV	Si	0.272 nm	0.575 nm

a : Inelastic mean free path of the Auger electron which is emitted from the atom A (in the A_XB_Y molecule) and travels in the matrix C.
b : Energy of the Auger electron which is emitted from the atom A (in the A_XB_Y molecule).

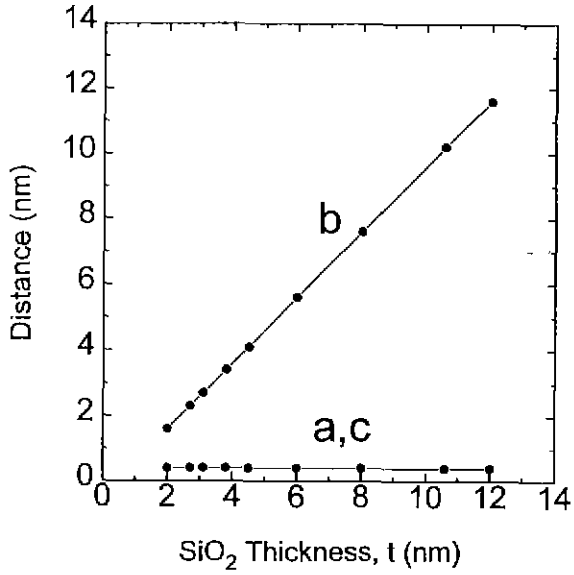

Fig. 5. Distances **a**, **b** and **c** which are defined in Fig. 4 as a function of SiO_2 thickness (t), showing that **a** is virtually equal to **c** regardless of the SiO_2 thickness and thus the thickness t of the interfacial SiO_2 layer can be represented by the FWHM of $R_{Si(Si_{2})}$.

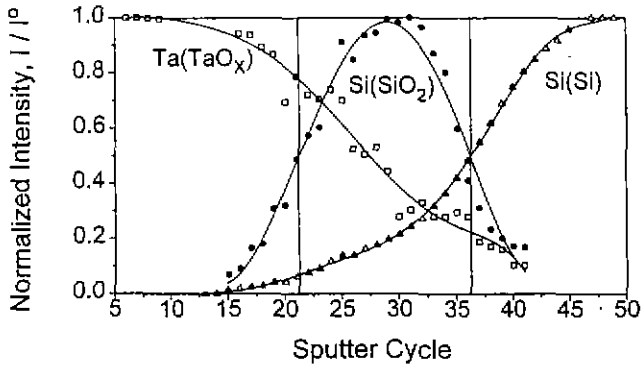

Fig. 6. Sputtered depth profile obtained from the specimen 1. One sputter cycle corresponds to the sputtered depth of 0.73 nm.

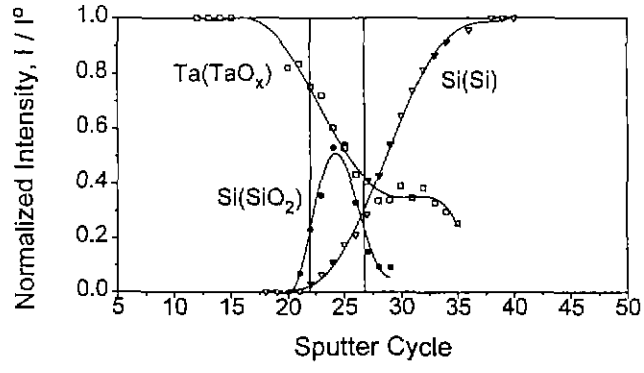

Fig. 7. Sputtered depth profile obtained from the specimen 2. One sputter cycle corresponds to the sputtered depth of 0.73 nm. The calculated thickness of the SiO_2 layer is 3.4 nm.

Auger electron of Ta atom in TaO_X was considered to lie halfway between $E_{Ta(Ta_2O_5)}$ (1674 eV) and $E_{Ta(Ta)}$ (1680 eV). The monolayer thickness A_{TaO_X} of the TaO_X matrix was also considered to lie halfway between $A_{Ta_2O_5}$ (0.229 nm) and A_{Ta} (0.262 nm).

Fig. 4 shows the theoretical depth profiles of the normalized intensities ($R_{Ta(TaO_X)}$, $R_{Si(SiO_2)}$ and $R_{Si(Si)}$) obtained from the calculated λ and $\cos\theta$ values when the thickness (t) of SiO_2 interfacial layer is 2.0 nm (X : 0 ~ 2.0 nm). The position Xs where the intensity shows the half maximum in the $R_{Si(SiO_2)}$ curve do not coincide with the surfaces of the SiO_2 layer because of the non-zero IMFP of Auger electrons. Those differences in position are denoted by **a** and **c** as shown in Fig. 4. The overlapped distance is denoted by **b**. The full width at half maximum (FWHM) of $R_{Si(SiO_2)}$ is **a+b**, whereas the thickness (t) of the interfacial layer is **b+c**. Fig. 5 shows the variations of **a**, **b** and **c** with the thickness of SiO_2 layer. Note that **a** is virtually equivalent to **c** with a value of 0.4 nm regardless of the SiO_2 thickness. As a result, the FWHM obtained from the sputtered depth profiles can be regarded as the thickness of SiO_2 interfacial layer formed between Ta_2O_5 thin film and Si substrate.

2. Sputtered depth profiles

Figs. 6 and 7 are the sputtered depth profiles acquired experimentally from the specimens 1 and 2, respectively. The shapes of the sputtered depth profiles are somewhat different from those of the theoretical ones because of the preferred sputtering, atomic mixing effects and surface roughness induced by ion sputtering. One sputter cycle in the Figs. represents the Ar ion sputtering for 6 seconds. The sputtered depth of the interfacial SiO_2 layer per sputter cycle was obtained by dividing the thickness (10.9 nm) of the SiO_2 interfacial layer of specimen 1 by the sputter cycles (14.9 cycle) corresponding to FWHM of $R_{Si(SiO_2)}$. The sputtering rate obtained was 0.73 nm/cycle. The thickness of the interfacial SiO_2 layer of specimen 2

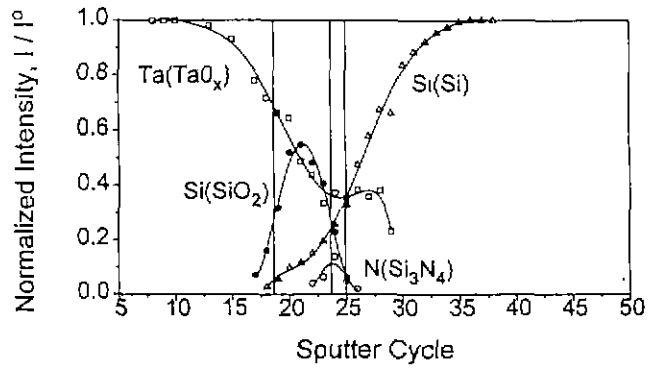

Fig. 8. Sputtered depth profile obtained from the specimen 3 that has a SiO_2/Si_3N_4 double interfacial layer. One sputter cycle corresponds to 0.73 nm. The calculated thicknesses of the SiO_2 layer and the SiO_2/Si_3N_4 double layer were 3.7 nm and 4.6 nm, respectively.

Table 3. Thicknesses of the Interfacial Layers Measured by the Cross-Sectional TEM and the AES Depth Profiling.

	Cross-Sectional TEM	AES depth profiling
Specimen 1	SiO_2 : 10.9 nm[a]	SiO_2 : 10.9 nm
Specimen 2	SiO_2 : 3.1 nm	SiO_2 : 3.4 nm
Specimen 3	SiO_2/Si_3N_4 : 4.2 nm[b]	SiO_2 : 3.7 nm
		SiO_2/Si_3N_4 : 4.6 nm

a : This thickness is used as a reference value to determine the sputtering rate of the SiO_2 layer during AES depth profiling.
b : SiO_2 layer is not distinguishable from the Si_3N_4 layer in the corss-sectional TEM examination.

can be determined by multiplying the sputter cycles (4.7 cycle) corresponding to FWHM of $R_{Si(Si_3N_4)}$ by the sputtering rate (0.73 nm/cycle). The calculated thickness (3.4 nm) of specimen 2 is found to be overestimated by about 10%, comparing with the value (3.1 nm) determined by the high resolution cross-sectional TEM micrograph of Fig. 2(b).

Fig. 8 shows the sputtered depth profile obtained from the specimen 3 having a SiO_2/Si_3N_4 double interfacial layer. In AES spectra, the LMM peak of Si in Si_3N_4 was not distinguishable from that of Si in Si single crystal. Thus, we monitored N KLL Auger peak (379 eV) instead of Si LMM peak for the detection of Si_3N_4 phase. The depth profile of Si_3N_4 was represented by $R_{N(Si_3N_4)}$. In the AES profile, SiO_2 and Si_3N_4 are distinguishable from each other. A large part of the Si_3N_4 layer on Si substrate was found to be converted into SiO_2 layer during the deposition of Ta_2O_5 film because of the strong oxidation power of the ECR oxygen plasma. This means that Si_3N_4 layer is not a proper buffer layer for the ECR PECVD system. The FWHM of $R_{Si(SiO_2)}$ corresponds to 5.0 sputter cycles, which gives a SiO_2 layer thickness of 3.7 nm. The FWHM of $R_{N(Si_3N_4)}$ corresponds to 2.4 sputter cycles, which gives a Si_3N_4 layer thickness of 1.8 nm assuming the same sputtering rate as for SiO_2. The total thickness of the SiO_2/Si_3N_4 double interfacial layers is 4.6 nm, which is also overestimated by about 10% comparing with the value (4.2 nm) determined by the cross-sectional TEM micrograph of Fig. 2(c). The resulted values were summarized in Table 3. It is believed that this overestimation of the thicknesses of specimens 2 and 3 is due to the broadening of the AES depth profiles. The broadening may come from the atomic mixing and the sputtering induced surface roughness, which have a more important effect for the thinner layer. Nevertheless, the thickness measured by the AES depth profiling technique agreed reasonably well, within 10%, with those measured by the cross-sectional TEM. Furthermore, the AES depth profiling can effectively discriminate the two mixed amorphous layers, which is unattainable with TEM examination.

IV. Conclusions

Theoretical calculation of AES depth profiles was performed by considering the inelastic mean free path of Auger electrons and angular acceptance function of CMA. Comparing the theoretical depth profiles with the sputtered ones could afford the quantitative analysis of the ultrathin interfacial SiO_2 and Si_3N_4 layers. The thicknesses measured by the AES depth profiling technique agreed reasonably well with those determined by the high resolution cross-sectional TEM. Furthermore, the mixed layer of SiO_2 and Si_3N_4, which were not distinguishable from each other under TEM examination, could be effectively analyzed. It has been shown that the AES depth profiling is a convenient tool for the quantitative analysis of the ultrathin interfacial layer, permitting the analysis within a reasonable timespan without any special process in preparing the analysis sample.

Acknowledgments

This research was sponsored by Samsung Electronics Co. Ltd. and by Korea Science and Engineering Foundation through Research Center for Thin Film Fabrication and Crystal Growing of Advanced Materials.

References

1. P. L. Young, "DC Electrical Conduction in Thin Ta_2O_5 Films, II. Highly Imperfect Films," *J. Appl. Phys.*, **47**, 242-247 (1976).
2. Y. Nishioka, H. Shinriki and K. Mukai, "Influence of SiO_2 at the Ta_2O_5/Si Interface on Dielectric Characteristics of Ta_2O_5 Capacitors," *J. Appl. Phys.*, **61**, 2335-2341 (1987).
3. I. Kim, S. D. Ahn, B. W. Cho, S. T. Ahn, J. Y. Lee, J. S. Chun and W. J. Lee, "Microstructure and Electrical Properties of Tantalum Oxide Thin Film Prepared by Electron Cyclotron Resonance Plasma Enhanced Chemical Vapor Deposition," *Jpn. J. Appl. Phys.*, **33**, 6691-6698 (1994).
4. H. J. Mathieu and D. Landolt, "AES Sputter Profiling and Angle Resolved XPS of In Situ Grown Very Thin Tantalum Oxide Films," *Surf. Interface Anal.*, **6**, 82-89 (1984).
5. M. P. Seah and W. A. Dench, "Quantitative Electron Spectroscopy of Surfaces," *Surf. Interface Anal.*, **1**, 2-11 (1979).
6. S. Hofmann and J. M. Sanz, "Quantitative XPS Analysis of the Surface Layer of Anodic Oxides Obtained During Depth Profiling by Sputtering with 3keV Ar^+ Ions," *J. Trace and Microprobe Tech.*, **1**, 213-264 (1982).